Urolithin A ameliorates experimental autoimmune encephalomyelitis by targeting aryl hydrocarbon receptor

Pei-Xin Shen[1], Xing Li[1], Si-Ying Deng[1], Li Zhao[1], Yan-Yan Zhang, Xin Deng, Bing Han, Jie Yu, Yin Li, Zhe-Zhi Wang, Yuan Zhang*

National Engineering Laboratory for Resource Development of Endangered Crude Drugs in Northwest China, The Key Laboratory of Medicinal Resources and Natural Pharmaceutical Chemistry, The Ministry of Education, College of Life Sciences, Shaanxi Normal University, Xi'an, Shaanxi 710119, The People's Republic of China

ARTICLE INFO

ABSTRACT

Background: Urolithin A (URA) is an intestinal microbiota metabolic product from ellagitannin-containing foods with multiple biological activities. However, its role in autoimmune diseases is largely unknown. Here, for first time, we demonstrate the therapeutic effect of URA in an experimental autoimmune encephalomyelitis (EAE) animal model.
Methods: Therapeutic effect was evaluated via an active and passive EAE animal model *in vivo*. The function of URA on bone marrow-derived dendritic cells (BM-DCs), T cells, and microglia were tested *in vitro*.
Findings: Oral URA (25 mg/kg/d) suppressed disease progression at prevention, induction, and effector phases of preclinical EAE. Histological evaluation showed that significantly fewer inflammatory cells, decreased demyelination, lower numbers of M1-type microglia and activated DCs, as well as reduced infiltrating Th1/Th17 cells were present in the central nervous system (CNS) of the URA-treated group. URA treatment at 25 μM inhibited the activation of BM-DCs *in vitro*, restrained Th17 cell differentiation in T cell polarization conditions, and in a DC-CD4$^+$ T cell co-culture system. Moreover, we confirmed URA inhibited pathogenicity of Th17 cells in adoptive EAE. Mechanism of URA action was directly targeting Aryl Hydrocarbon Receptor (AhR) and modulating the signaling pathways.
Interpretation: Collectively, our study offers new evidence that URA, as a human microbial metabolite, is valuable to use as a prospective therapeutic candidate for autoimmune diseases.

1. Introduction

Multiple Sclerosis (MS) is a kind of neurodegenerative disease in which the abnormally activated immune cells attack the Central Nervous System (CNS). The disease is characterized by inflammatory cell infiltration and demyelination. Clinical symptoms mainly include optic nerve dysfunction, diplopia, limb sensation or movement disorder, and ataxia [1−3]. The prevalence of MS varies from region, and its therapeutic mechanism has not been thoroughly studied. Recently, researchers claim that it may be related to genetic factors, viral infection, environmental factors, and autoimmunity etc [4]. This disease is common in young and middle-aged groups, with high disability rate. Cases are distributed throughout the world, the development of immunotherapies that act on MS has allowed for a substantial reduction in CNS inflammation and relapse rate during the past two decades. However, existing drugs are largely insufficient to prevent the accumulation of permanent disability from axonal and neuronal damage and loss [5]. Experimental autoimmune encephalomyelitis (EAE) is the most widely used animal model because of its similar pathological features and disease progression to MS.

Previous studies have demonstrated that multiple types of immune cells participate in the pathogenesis of EAE, especially dendritic cells (DCs) and CD4$^+$ T Cells. Dendritic cells, as the most powerful professional antigen-presenting cells, are widely present in various lymphoid organs and the blood circulation system of the body. Dendritic cells can specifically recognize antigen peptides and present them to naïve T cells, which stimulate the activation of naïve T cells [6, 7]. In addition, the selective depletion of a subset of classical

Research in context

Evidence before this study

Multiple Sclerosis (MS) is characterized by inflammatory cell infiltration and demyelination. It was generally accepted that helper T cell subsets, Th17 cells, were pro-inflammatory cell groups proven to be responsible for inducing autoimmune diseases and inflammatory processes. In recent years, the application of plant-derived natural anti-inflammatory compounds in autoimmune diseases has attracted attention and achieved certain results.

Added value of this study

In this study, we demonstrated that URA had significant preventive and therapeutic effects on MOG35-55-induced EAE mice at different disease stages, and remarkably reduced mononuclear cells (MNCs) in the central nervous system (CNS), while the immune response in the periphery were mildly affected. URA treatment suppressed the activation of bone marrow-derived dendritic cells (BM-DCs) in vitro, inhibited pro-inflammatory factor secretion of SIM-A9 microglia, as well as dampening Th17 cell differentiation. Furthermore, we confirmed the weak pathogenicity of URA-treated MOG-specific Th17 cells via an adoptive transfer model. Mechanistic study revealed that the inhibition effect of URA on Th17 differentiation was AhR-dependent.

Implications of all the available evidence

Our data indicates that URA - with its wide spectrum of pharmacological activities, low cost, and abundant sources - has encouraging therapeutic potential for the treatment of autoimmune diseases such as MS.

dendritic cells present in the naïve central nervous system reduces the incidence of EAE [8], indicating that DCs are expected to be potential therapeutic target for MS. For CD4$^+$ T Cells, it is generally accepted that regulatory T cells (Tregs) have protective and antiphlogistic effects, while helper T cell subsets, Th1 and Th17 cells, are pro-inflammatory cell groups that have been proved to be responsible for inducing autoimmune diseases and inflammatory processes [9−12]. Although the pathogenic mechanism is partially known, and there are different drugs for the treatment of MS in the clinic, it is difficult to avoid side effects and risks [13]. In recent years, the application of plant-derived natural anti-inflammatory compounds in autoimmune diseases has attracted attention and achieved certain results [14−16]. Natural products are huge reserves of candidate drugs for autoimmune diseases due to their wide sources and rich species diversity.

Urolithin A (URA) is the biotransformation of ellagic acid through the intestinal microbiota. Ellagic acid is derived from a variety of fruits or nuts, such as pomegranate, strawberry, grape, and pecan, and it also produced by some medicinal plants like *Geranium pratense* L., *Geum urbanum* L., and *Potentilla anserina* L. [17−20]. A study has reported that after intestinal metabolism and circulation, URA is present in the plasma at the concentrations of 4−18 μM, and can be in the systemic circulation for up to 72 h [21]. URA not only reduced levels of activated microglia and astrocytes, but also reduced amyloid fibrosis deposition in the animal model of Alzheimer's disease [22]. Research by DaSilva et al. also confirmed that URA can inhibit neuroinflammation in BV2 microglia stimulated by LPS [23]. Existing evidence indicates the potential of URA in treating autoimmune diseases; however, more direct evidence is needed to prove the beneficial effects and molecular mechanism of URA in autoimmunity. Here, we used the EAE model to demonstrate that URA can inhibit the infiltration of dendritic cells and pathogenic T cells

into the CNS, suppress the inflammatory factors IL-17, IFN-γ, and increase the number of Tregs to effectively alleviate the disease process. The therapeutic efficacy of URA in EAE makes it conceivable to identify the signaling pathways implicated in the regulatory actions of URA and provide more clues for natural-source diet therapy for the treatment autoimmune disorders.

2. Methods

2.1. Mice and ethics

Eight to twelve week-old C57BL/6 female mice weighing 18−20 g were purchased from Air Force Military Medical University, Xi'an, China. IL-17A-IRES-GFP mice (Stock No: 018472) and 2D2 TCR transgenic mice (Stock No: 006912) were purchased from the Jackson Laboratory. The mice were fed under standard light and temperature conditions, and free access to water and food. All animal experiments were approved by the institutional animal care committee of Shaanxi Normal University, and in accordance with the approved institutional guidelines and regulations (No. ECES-2015-0247).

2.2. EAE induction, treatment, and drug dissolution

EAE induction and scoring rules followed previous studies [24]. URA was purchased from (Ark Pharm, Inc, 1143-70-0). CH-223191 was purchased from MCE (301326-22-7) and dissolved in dimethyl sulfoxide (DMSO, Sigma Aldrich, 67-68-5). URA was dissolved in a specific solvent, and the solvent (Vehicle) consisted of DMSO (3%, Sigma Aldrich, 67-68-5), Kolliphor-EL (10%, Sigma Aldrich, 61791-12-6) and 5% (w/v) Dextrose solution (87%, Sigma Aldrich, 50-99-7). The stock was diluted into different concentrations, and administered orally to EAE mice at 10, 25, or 50 mg/kg/d after immunization.
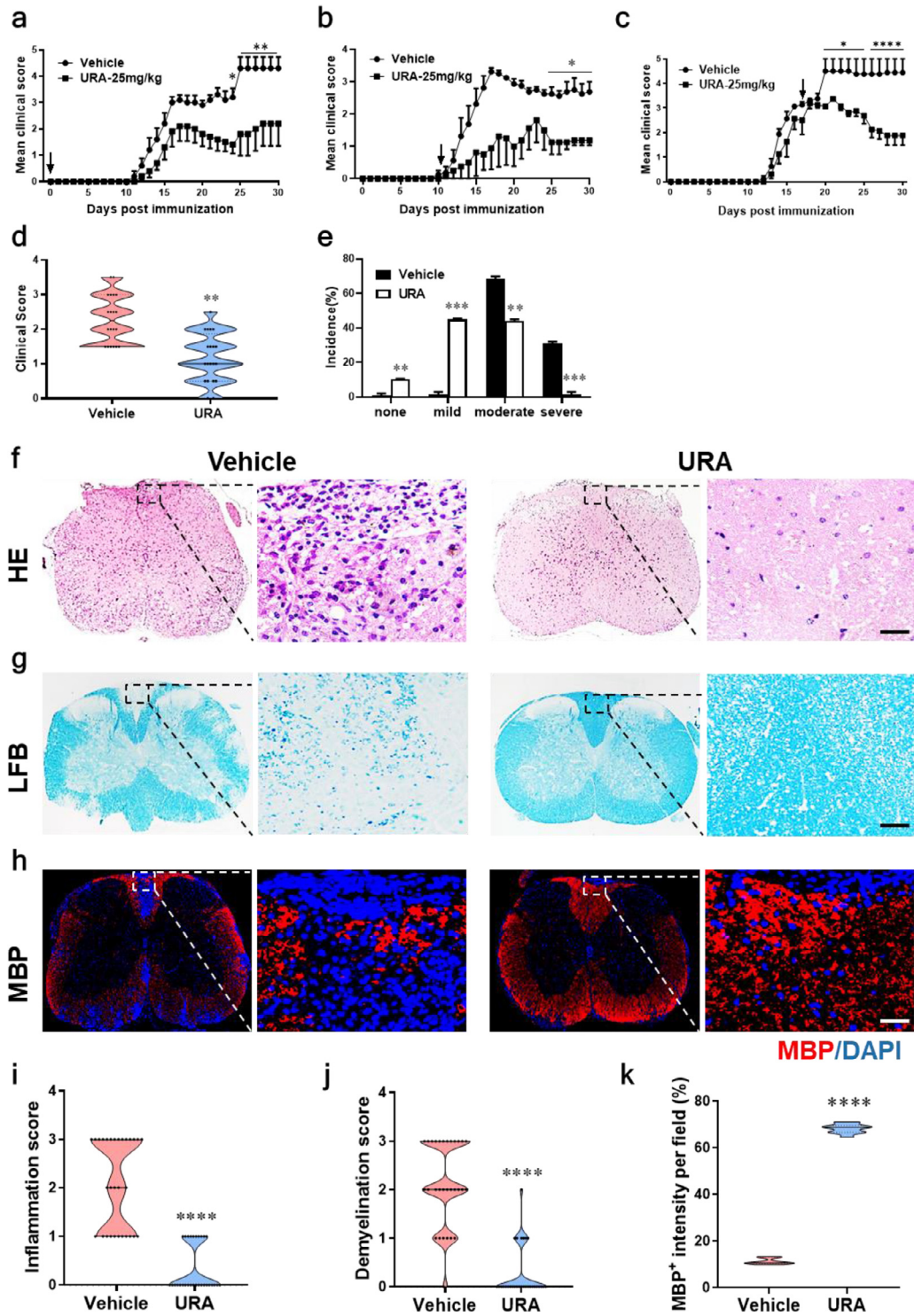
2.3. Immunohistopathology

Mice were sacrificed at day 20 p.i. (the acute phase of EAE mice). Approximately 0.5 cm of the lumbosacral enlarged spinal cord was removed from the sacrificed mouse and fixed in 4% (w/v) paraformaldehyde. Paraffin-embedded sections (6 μm) of spinal cords and brain were stained with hematoxylin and eosin (H&E) or luxol fast blue (LFB) and examined by light microscopy (Nikon, Japan). Frozen embedded sections (8 μm) of the spinal cord were fixed, eluted, incubated with antibodies, and mounted, and then imaged and analyzed by an upright fluorescence microscope (Leica, Germany). H&E staining [25] was used to evaluate inflammation by blind evaluation: 0, none; 1, a small number of inflammatory cells; 2, tissue perivascular infiltration; 3, a rich perivascular cuff-like extension to adjacent tissues. Demyelination is evaluated by LFB staining: 0, none; 1, rare lesions; 2, several areas of demyelination; 3, large (confluent) demyelinated areas.

2.4. Isolation of CNS mononuclear cells (MNCs)

Brain and spinal cord were excised from C57BL/6 mice immunized with MOG$_{35-55}$ (Genscript, 163913-87-9), mechanically minced the tissue in a petri dish. Neural Tissue Dissociation Kit (Miltenyi Biotec, 130-092-628) formulated solution I: Enzyme P 50 μL + Buffer X 1900 μL (per mouse), and solution II: Enzyme A 10 μL + Buffer Y 20 μL (per mouse). Tissues were repeatedly digested for isolating CNS mononuclear cells in a shaker at 37°C, 70 rpm for 15 min. The above dissociated cells were passed through a 70 μm nylon mesh and the filter was rinsed with Vehicle. After centrifugation at 300 g for 10 min, the resulting cell pellet was blown off, and subjected to gradient centrifugation with 70% and 30% percoll (GE Healthcare, 17-0891-09). Both the rate of increase and decrease were adjusted to 1. Then the dropper was inserted into the middle of the two liquid layers to slowly aspirate about 15 mL to obtain mononuclear cells (MNCs).

Fig. 1. *URA Alleviated the Development of Experimental Autoimmune Encephalomyelitis (EAE).* C57BL/6 mice were administered orally with vehicle (•) or URA (25mg/kg, □) daily at the day of EAE induction (a), day 11 p.i. (b), and day 17 p.i. (c). EAE development were evaluated and recorded following a 0−5 scale. (d) Distribution of disease status and (e) incidence of disease severity at the end points of experiment (day 30 p.i.). EAE mice classify as severe disease severity rating (clinical score ≥3), moderate (clinical score 1.5-2.5), mild (Clinical score <1.5) or none (no clinical symptoms). URA- or vehicle-treated EAE mice were sacrificed at day 30 p.i., and spinal cords were harvested. Sections at lumbar level (L3) were analyzed by (f) H&E and (g) LFB. (h) Immuno-labeling for myelin basic protein (MBP) was used to determine the percentage of myelinated areas within a lesion (defined in the DAPI channel as nuclei). (i) Mean score of inflammation in H&E staining. (j) Quantification of demyelination area and (k) MBP intensity was measured in the lesion areas in the white matter of the lumbar spinal cord using Image-Pro. Scale bar = 50 μm. n = 5 mice each group. Symbols represent mean ± SEM. Data from three independent experiments. $^{**}p < 0.01$, $^{***}p < 0.001$, $^{****}p < 0.0001$, as determined by two-way ANOVA analysis (a−c) or unpaired Student's t test (d, e, i-k).

2.5. Flow cytometry analysis

CNS-infiltrating MNCs or splenocytes were suspended in complete RPMI 1640 with 10% FBS at a density of 2 × 10^6 cells/mL, then were stimulated with 10 and 25 μg/mL MOG peptide for overnight or 72 h, respectively. Cells were incubated with fluorochrome-conjugated Abs to CD45 (BD, 552848), CD11b (BD, 552848), CD11c (BD, 565452), CD80 (eBioscience, 17-0801-81), CD86 (BD, 561963), MHCII
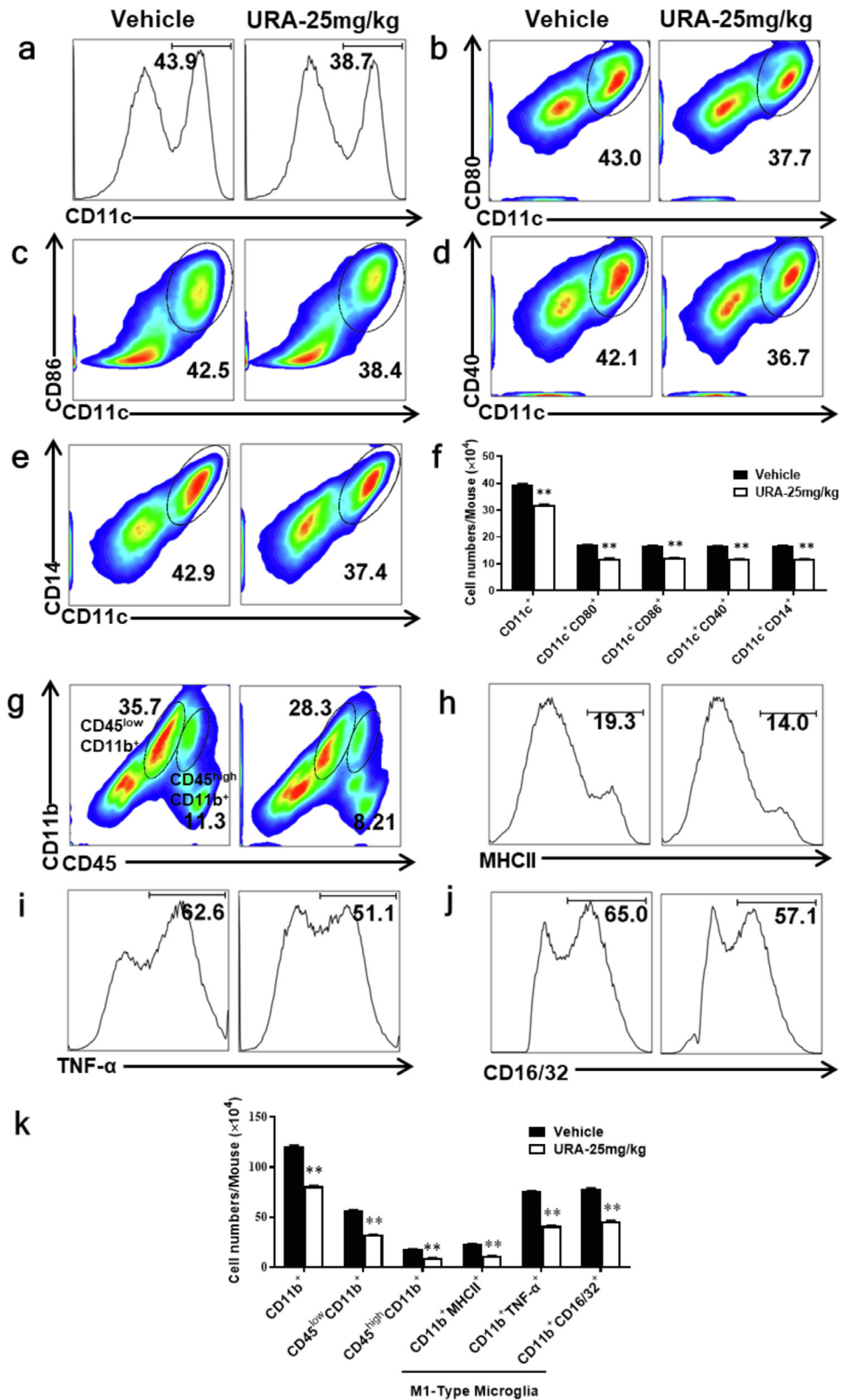
Fig. 2. *URA Inhibited the Activation of Dendritic Cells and Microglia in CNS.* Mice were treated with vehicle or URA (25 mg/kg) on the day of EAE induction and sacrificed at day 20 p.i. Spinal cords and brains were harvested and mononuclear cells (MNCs) isolated, following stimulation with MOG_{35-55} (25 μg/mL) for 24 h. (a) Percentage of $CD11c^+$ cells infiltrated into CNS in URA- or vehicle-treated group. Frequencies of $CD11c^+ CD80^+$ (b), $CD11c^+ CD86^+$ (c), $CD11c^+ CD40^+$ (d), $CD11c^+ CD14^+$ (e) cells were assessed by flow cytometry. (f) Absolute numbers of infiltrated $CD11c^+$ cells were calculated by multiplying the percentages of these cells with total numbers of MNCs in each group. (g) The percentage of $CD45^{high}$ $CD11b^+$, $CD45^{low}$ $CD11b^+$, and $CD11b^+ MHCII^+$ (h), $CD11b^+ TNF-\alpha^+$ (i), $CD11b^+ CD16/32^+$ (j) cells in Vehicle- or URA-treated EAE mice. (k) Absolute numbers of infiltrated $CD11b^+$ cells. Data represent three independent experiments and symbols represent mean ± SEM. Data were determined by unpaired Student's t test, **p < 0.01.
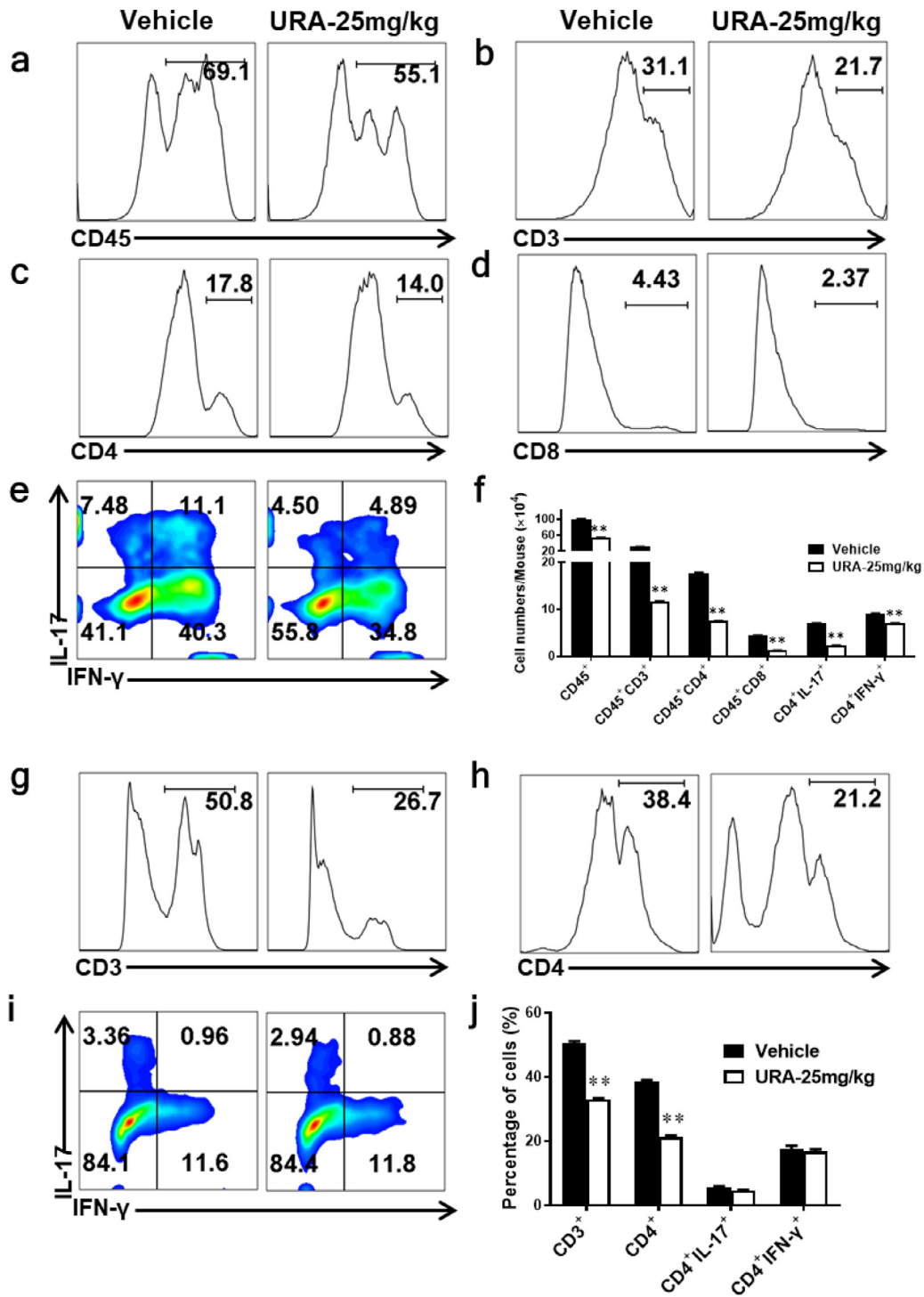
Fig. 3. *URA Suppressed the Infiltration of Pathogenic T Cells from the Periphery to CNS.* The percentage of CD45$^+$ (a), CD45$^+$ CD3$^+$ (b), CD45$^+$ CD4$^+$ (c), CD45$^+$ CD8$^+$ (d) cells in Vehicle- or URA- treated EAE mice. MNCs were harvested from spinal cords and brains. (e) Frequencies of CD4$^+$ IL-17$^+$ and CD4$^+$ IFN-γ^+ cells infiltrated into CNS. (f) Absolute cell counts infiltrated into CNS in a-e. (g-i) The percentages of CD3$^+$ (g), CD4$^+$ (h) and CD4$^+$ IL-17$^+$/CD4$^+$ IFN-γ^+ cells (i) isolated from spleen and stimulated with MOG$_{35-55}$ (25 μg/mL) for 72 h. (j) Statistics on the relative proportion of cells in g-i. Data represent three independent experiments, n = 5 mice per group. Symbols represent mean $\pm$ SEM. Unpaired Student's t test, $^{**}p < 0.01$.

(BD, 553623), CD14 (BD, 740357), CD16/32 (BD, 561727), CD3 (BD, 564378), CD4 (BD, 553051), or isotype control Abs (BD Biosciences, San Jose, CA) for 30 min on ice for surface-marker staining. For intracellular cytokine staining, cells were stimulated with phorbol 12-myristate 13-acetate (50 ng/mL, Sigma Aldrich, P8139) and ionomycin (500 ng/mL, Sigma Aldrich, 13909) in the presence of GolgiPlug (1 mg/10^6 cells, BD, 555029) for 4 h. The staining procedure was performed following a previously described protocol [26]. Flow

cytometric analysis performed on CytoFLEX (Beckman Coulter Eurocenter S.A.) and data were analyzed with FlowJo software (Treestar, Ashland, OR).

2.6. The preparation of BM-DCs

For isolation of the immature bone marrow precursors, femurs and tibias were removed under sterile conditions from naïve C57BL/6
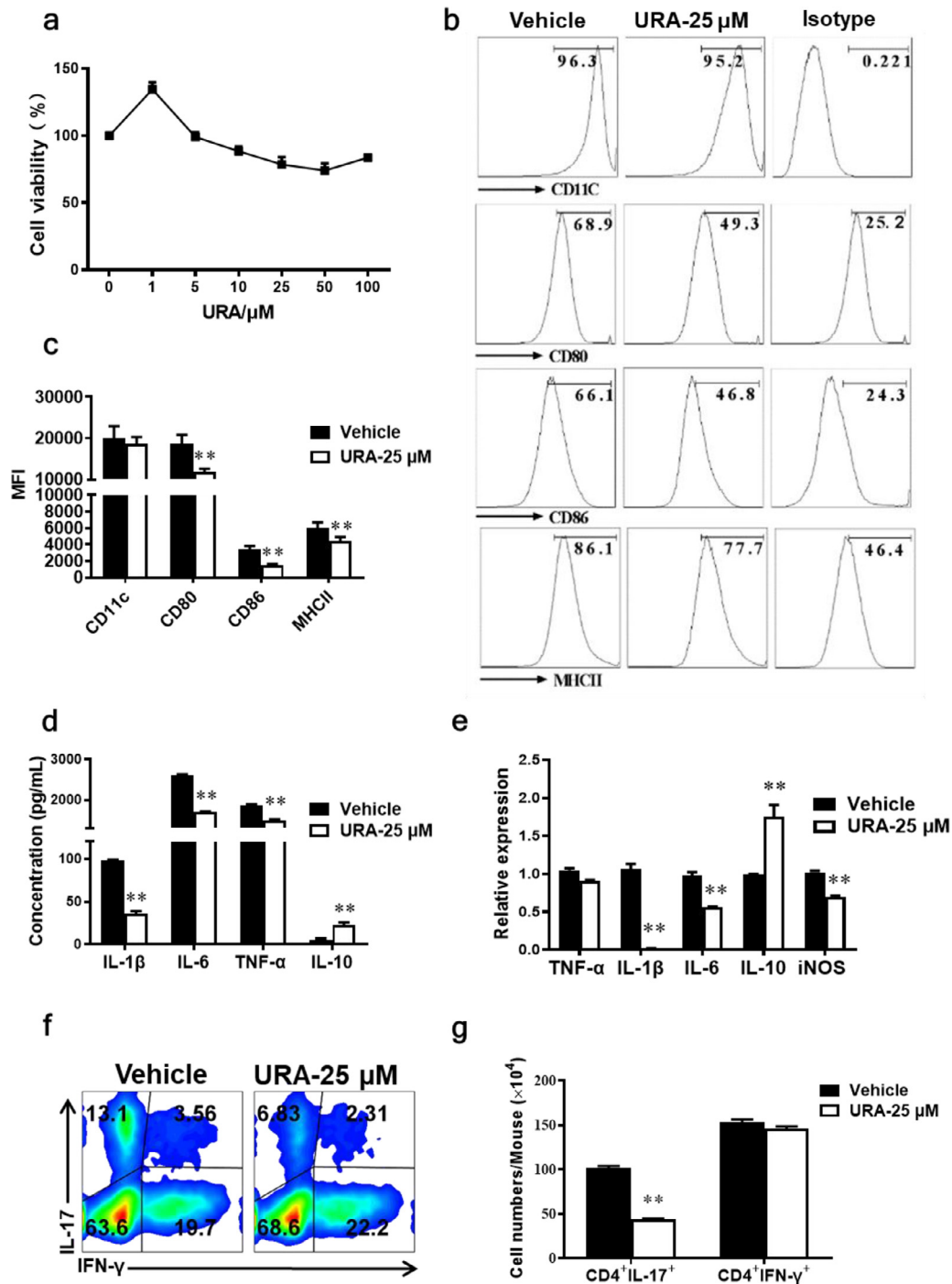
Fig. 4. *URA Inhibited Activation of Bone Marrow-Derived Dendritic Cells (BM-DCs) in vitro.* Primary BM-DCs were generated from femurs and tibias of naïve C57BL/6 mice, and stimulated with 100 ng/μL LPS, and cultured with URA at 25 μM for 18 h. (a) Cell viability of BM-DCs treated with URA (1-100 μM) was detected by MTS assay. (b) CD11c^{+}, CD80^{+}, CD86^{+}, MHCII^{+} cells were gated in the CD11c^{+} cells and analyzed using flow cytometry. (c) Median Fluorescence Intensity (MFI) statistics of CD11c^{+}, CD80^{+}, CD86^{+}, and MHCII^{+} cells. (d) Supernatants derived from BM-DCs cultures were analyzed for the level of indicated cytokines by ELISA. (e) Expression of indicated genes from BM-DCs were determined at 4 h by real time-Quantitative PCR under 25 μM URA treatment. (f) Naïve CD4^{+} cells were cocultured with BM-DCs pretreated with or without URA. (g) The absolute numbers of CD4^{+} IFN-γ^{+}, CD4^{+} IL-17^{+} cells. Symbols represent mean ± SEM, unpaired Student's t test, **$p < 0.01$. One representative of three independent experiments is shown.

mice aged 8-12 weeks. After separating the muscle tissues around the femurs and tibias, the bone marrow precursors were flushed out of the bone marrow cavity with precooled PBS. Cells were filtered with a 100 μm nylon mesh, then cultured with RPMI1640 medium (SIGMA, R8758) containing 10 ng/mL of GM-CSF (PeproTech, 315-03), which was replaced every 3 days. After 9 days, bone marrow-derived dendritic cells (BM-DCs) were collected and cultured with GM-CSF-free medium for subsequent experiments.

2.7. In vitro T cell differentiation

Single-cell suspensions were isolated from the spleen of 2D2 TCR transgenic mice then cultured for 3 days with MOG$_{35-55}$ (25 μg/mL), soluble anti-CD3 (0.5 μg/mL, Bio X Cell, BE0002), anti-CD28 (1 μg/mL, Bio X Cell, BE0015-5), IL-6 (20 ng/mL, R&D, 406-ML-025), TGF-β (2 ng/mL, R&D, 7666-MB-005), IL-1β (10 ng/mL, R&D, 401-ML-010), anti-IFN-γ (10 μg/mL, Bio X Cell, BE0054), and anti-IL-4 (10 μg/mL,
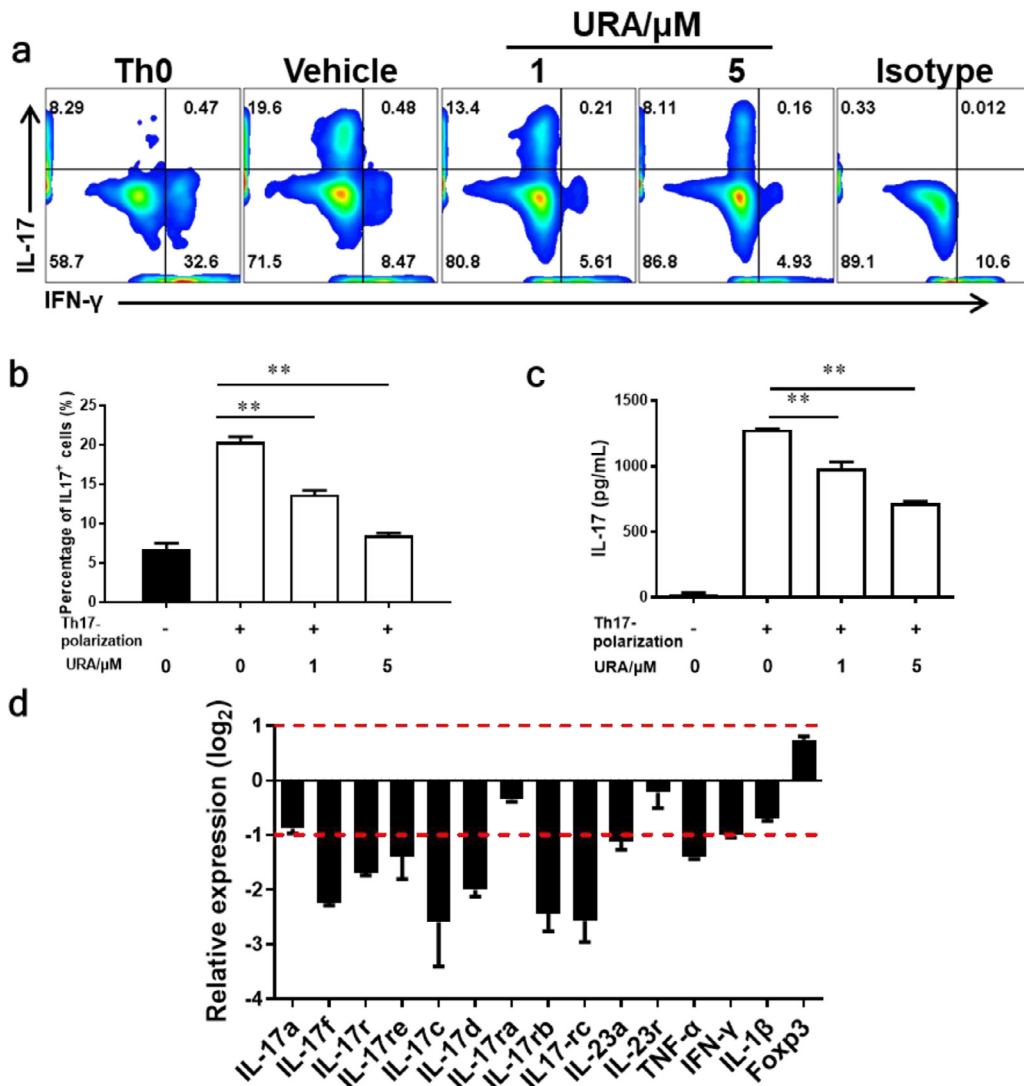
Fig. 5. *URA Restricted Th17 polarization in vitro.* (a) Effect of 1 and 5 μM URA on differentiation of TCR^{MOG} 2D2 T cell was analyzed using flow cytometry under Th17 polarization *in vitro.* (b) The percentage of Th17 cells in the CD4$^+$ subset was analyzed by intracellular staining of IL-17. (c) Supernatants derived from Th17 cell cultures were analyzed for the level of IL-17 production. (d) Relative expression of Th17 family genes of Th17 cells under URA treatment (5 μM). The relative expression was calculated by log2 of $-\Delta\Delta$Ct values from triplicate of PCR. Symbols represent mean $\pm$ SEM. Data were determined by unpaired Student's t test (b, c), **$p < 0.01$, ***$p < 0.001$.

Bio X Cell, BE0045) to induce differentiation into Th17 cells. Cells were analyzed by flow cytometry.

2.8. Adoptive transfer

For passive EAE, mice were euthanized 10 days after MOG$_{35-55}$ immunization, and spleen and lymph nodes were collected as previously described [27]. Single cells were incubated for 3 days in the presence of 25 μg/mL MOG$_{35-55}$, 10 ng/mL recombinant murine IL-23 (R&D, 1887-ML-010), and 2 ng/mL IL-2 (R&D, 402-ML-020) at 1×10^7 cells/mL. CD4$^+$ T cells were purified by CD4$^+$ T cell isolation kit and 1×10^6 cells per mouse were transferred via intravenous injection. Pertussis toxin (200 ng/mouse, List Biological Laboratories, 181) was injected intraperitoneally (i.p.) on days 0 and 2. EAE score was assessed by daily recording using a 0−5 scale.

2.9. Enzyme linked immunosorbent assay (ELISA)

Splenocytes were separated from Vehicle- or URA-treated EAE mice (incubated with 25 μg/mL of MOG$_{35-55}$ for 72 h), and supernatants were assembled for detection of IL-17 and GM-CSF with ELISA kits (R&D Systems, Minneapolis, MN). SIM-A9 microglia treated with

Vehicle or URA was inflamed with 100 ng/mL LPS for 18 h, and the microglia supernatant was collected and TNF-α production was assayed using ELISA kits according to manufacturer's instructions.

2.10. Real time-quantitative PCR

Total RNA was isolated using RNAprep Pure Cell/ Bacteria Kit (TIANGEN, DP430) and reverse transcribed with PrimeScript^{TM} RT Master Mix (Perfect Real Time) (TaKaRa, RR036A) according to the manufacturer's instructions. Messenger RNA expression was examined by real time-Quantitative PCR using 2 × ChamQ^{TM} SYBR$^®$ qPCR Master Mix (Vazyme, Q311-02). Data were quantitatively analyzed on Roche Molecular Biochemicals Light Cycler Software Version 3.5. Mouse GAPDH gene was used as endogenous control for sample normalization. Sequences of real time-Quantitative PCR primers are listed in Table S1.

2.11. Statistics

GraphPad Prism 8 (GraphPad, La Jolla, CA) was used for statistical analysis. Significant differences were evaluated by unpaired Student's t test or one-way ANOVA, except two-way ANOVA analysis used for
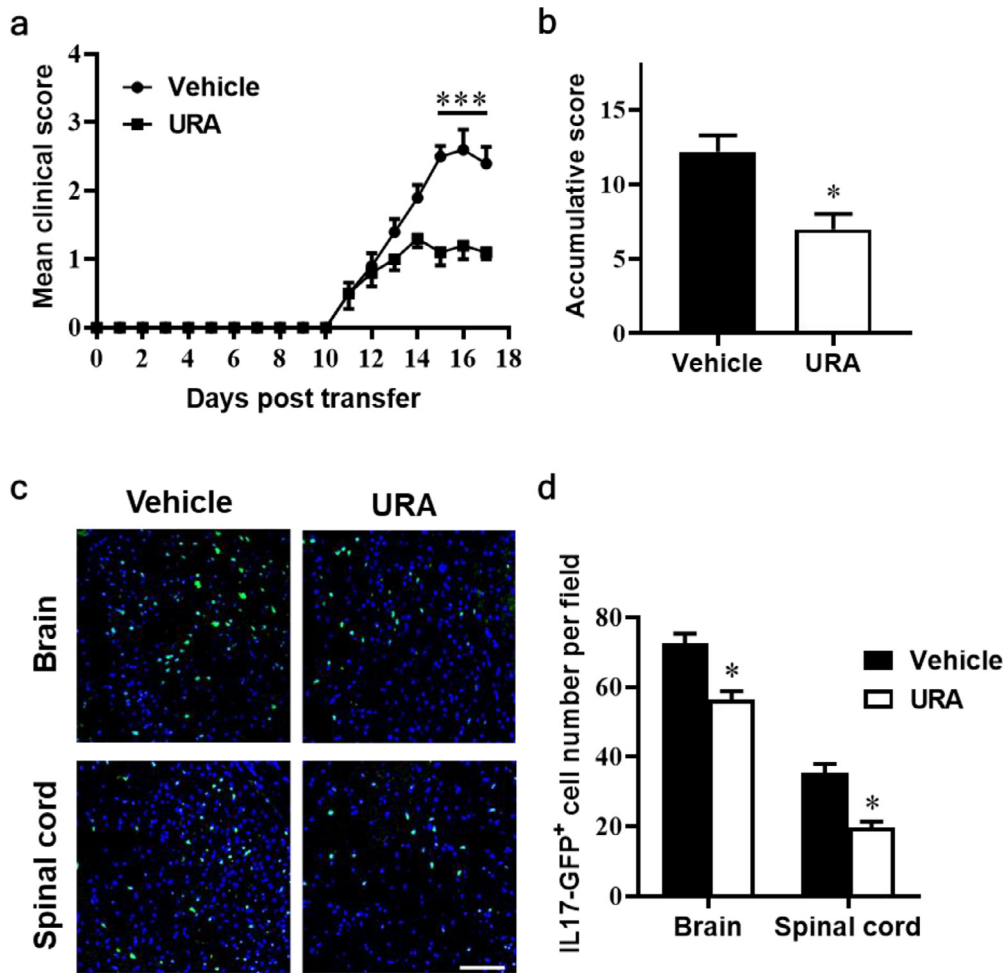
Fig. 6. *URA alleviated clinical disease development in a passive EAE model.* For passive EAE, cells were harvested from spleen and lymph nodes of IL-17A-IRES-GFP mice at day 10 p.i. MOG_{35-55} plus IL-23 and IL-2 were added into the culture medium in the presence or absence of 10 μM URA for 3 days. Purified $CD4^+$ cells were transferred to the naïve C57BL/6 recipient mice. (a) Mean clinical score of passive EAE. (b) Accumulative scores of passive EAE (sum of daily clinical scores from day 11 to day 17 p.t.). (c) Mice were sacrificed at day 17 after cell transfer, brain and spinal cords were subjected to fluorescence analysis of GFP^+ cells. (d) Statistical analyses of total GFP^+ cell numbers in (c) are shown. Scale bar = 100 μm. Symbols represent mean $\pm$ SEM (n = 5 each group) $^*p < 0.05$, $^{***}p < 0.001$, determined by two-way ANOVA (a), or nonparametric t test (c, d). One representative of two independent experiments is shown.

clinical score curves. Symbols represented as mean $\pm$ SEM, values of p less than 0.05 were considered significant.

2.12. Role of funding source

The funders had no role in study design, data collection, data analysis, interpretation, or writing of the report.

3. Results

### 3.1. URA effectively alleviated the clinical symptoms of EAE

In order to estimate the therapeutic effect of URA on EAE, 8~12-wk-old C57BL/6 female mice immunized with MOG_{35-55}/CFA were orally administered with URA under different doses. Results shown that 25mg/kg is the optimized dose to inhibit the progress of EAE, therefore this dose was selected for subsequent *in vivo* experiments. To further examine the effect of URA at different disease stages, URA was orally administered on the day of immunization (day 0 p.i.) and disease onset (day 11 p.i.) and peak (day 17 p.i.) respectively. The results showed that URA not only inhibited the disease course during prevention phase (Fig. 1a), but also significantly suppressed the development of EAE at the initial stage (Fig. 1b). Even at the peak of the disease, the clinical score was also greatly reduced (Fig. 1c). At the end time point at day 30

p.i., mice developed EAE which was divided into mild, moderate, and severe according to the degree of disease. URA-treated group significantly reduced disease severity of EAE mice (Fig. 1d, e). More than half of the mice in the URA-treated group had no disease characteristics or showed mild symptoms, while the vehicle group mainly exhibited moderate or severe disease (Fig. 1e). Mice were sacrificed at day 30 p.i, and the lumbosacral region of spinal cord was excised. Immunohistological analysis was performed for further assessing the effect of URA treatment on pathological changes in EAE mice. H&E and LFB staining results showed that the inflammatory infiltration and the demyelination of the white matter were more pronounced in the vehicle-treated group (Fig. 1f, g). Demyelinating lesions were also evaluated by the expression of myelin basic protein (MBP) in the spinal cord. Compared with the vehicle-treated mice, the proportion of intact myelin in the spinal cord of the URA-treated mice was significantly increased (Fig. 1h). Taken together, these results confirmed that URA substantially inhibited inflammatory cell infiltration and myelin depletion in EAE mice (Fig. 1i-k), indicated that URA had a considerable therapeutic effect in EAE.

3.2. URA treatment reduced CNS inflammation

As the most powerful professional antigen-presenting cells in the body, DCs play an important role in T cell activation and inflammation. The activation of DCs depended on the high expression of co-
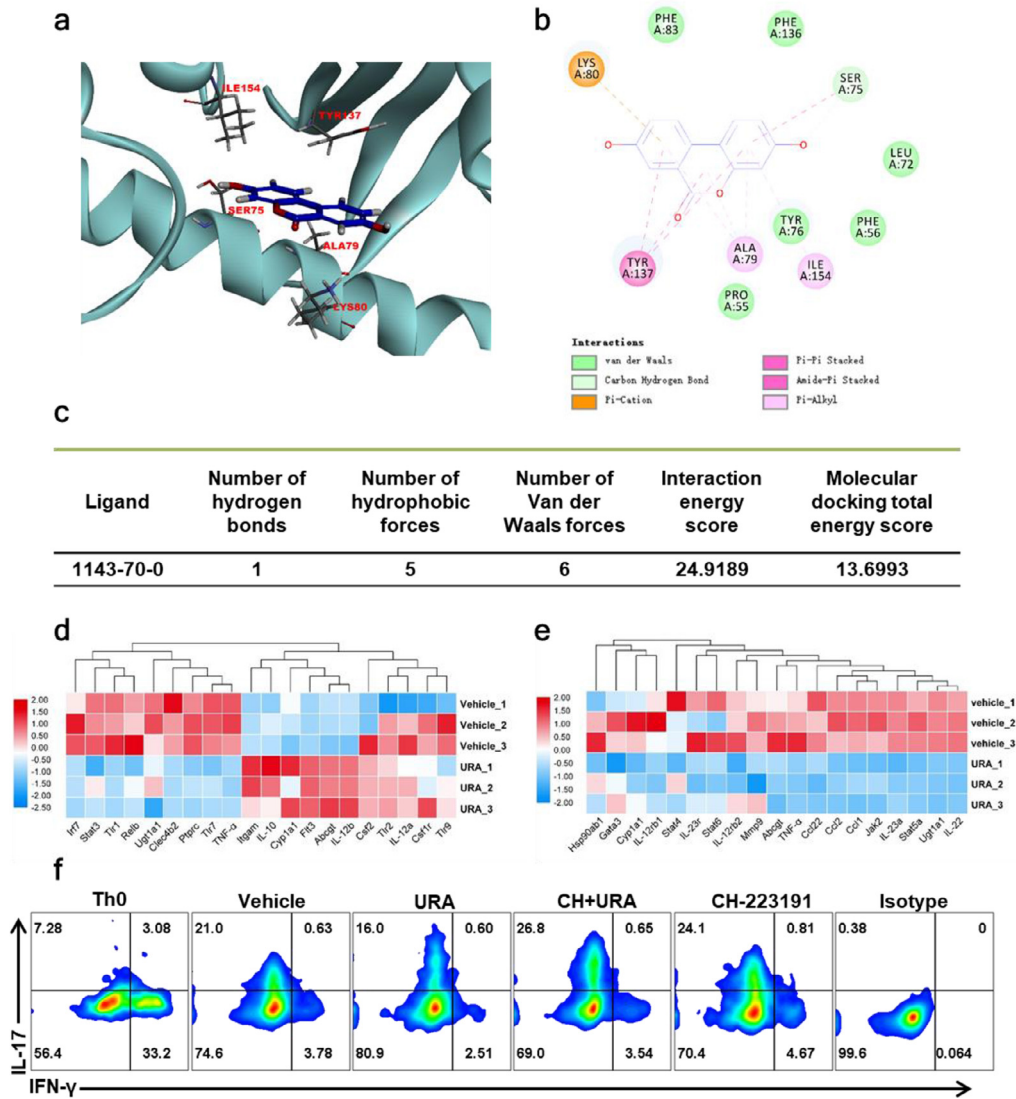
Fig. 7. *URA inhibited Th17 differentiation by targeting AhR in vitro.* (a) Molecular docking diagram of URA and AhR. (b) Schematic diagram of the interaction between URA and amino acid residues. (c) Statistical table of URA and AhR interaction and energy score. (d) Expression of AhR target genes in IL-17 Family Signaling Pathway in the presence or absence of 5 μM URA. (e) Expression of AhR target genes in dendritic cells developmental lineage pathway in the presence or absence of 5 μM URA. (f) Splenocytes from C57BL/6 mice were polarized under Th17 conditions for 3 days in the presence of either Vehicle or AhR antagonist (CH223191, 10 μM) or URA (2 μM) or pre-treated with 10 μM CH223191 for 4 h and subsequently treated cells with 2 μM URA. The induction of ex vivo IL-17 was measured by flow cytometry analysis. One representative of Three independent experiments is shown.

stimulatory molecules such as CD80, CD86, MHCII, thus activated DCs were shown to display strong immune stimulatory capacities [28]. To investigate the specific effects of URA treatment on DCs, CNS mononuclear cells (MNCs) in the URA or vehicle-treated group were isolated at day 20 p.i and incubated with MOG$_{35-55}$ (25 μg/mL). Cell phenotype was determined by flow cytometry 24 h later. Results shown that the proportion of CD11c$^+$ DCs infiltrating into the CNS was significantly lower than that of the control group (Fig. 2a). At the same time, the proportion of co-stimulatory molecules CD80, CD86, CD40, and CD14 expressed on CD11c$^+$ DCs were remarkably reduced (Fig. 2b-e). The absolute numbers of infiltrating cells described above were also significantly reduced (Fig. 2f). In addition, we analyzed the phenotype shift of microglia in the CNS of EAE mice under URA treatment. The percentage of CD45^{high}CD11b$^+$ cells (infiltrating macrophages and activated microglia), CD45^{low}CD11b$^+$ (microglia), and M1-type microglia (CD11b$^+$MHCII$^+$, CD11b$^+$TNF-α^+, and CD11b$^+$CD16/32$^+$ cells) populations were decreased obviously (Fig. 2g-j). The absolute numbers of activated microglia and macrophages infiltrating into CNS were decreased benefit from URA

treatment (Fig. 2k). These results demonstrated that URA treatment suppressed the activation of DCs and intrinsic microglia in CNS during EAE disease progression.

3.3. URA inhibited migration of pathogenic T cells from the periphery to CNS

Consistent with the effects observed by URA on dendritic cells and microglia, URA also decreased the percentages of pathogenic Th1/ Th17 cells. URA treatment resulted in a remarkable reduced in the percentage of CD45$^+$ (leukocytes), CD3$^+$ (total T lymphocytes), CD4$^+$ (helper T cells), and CD8$^+$ (cytotoxic T cells) cells infiltrating into the CNS (Fig. 3a-d). The percentage of Th1 and Th17 cells showed an obvious inhibition under URA treatment (Fig. 3e). Furthermore, the number of these cells was also dramatically reduced (Fig. 3f).

Consistent to the reduction of T cells numbers detected in the CNS, the proportion of CD3$^+$ and CD4$^+$ cells in the URA-administered group was also remarkably reduced in the peripheral immune system (Fig. 3g, h). However, no significant differences were observed in the
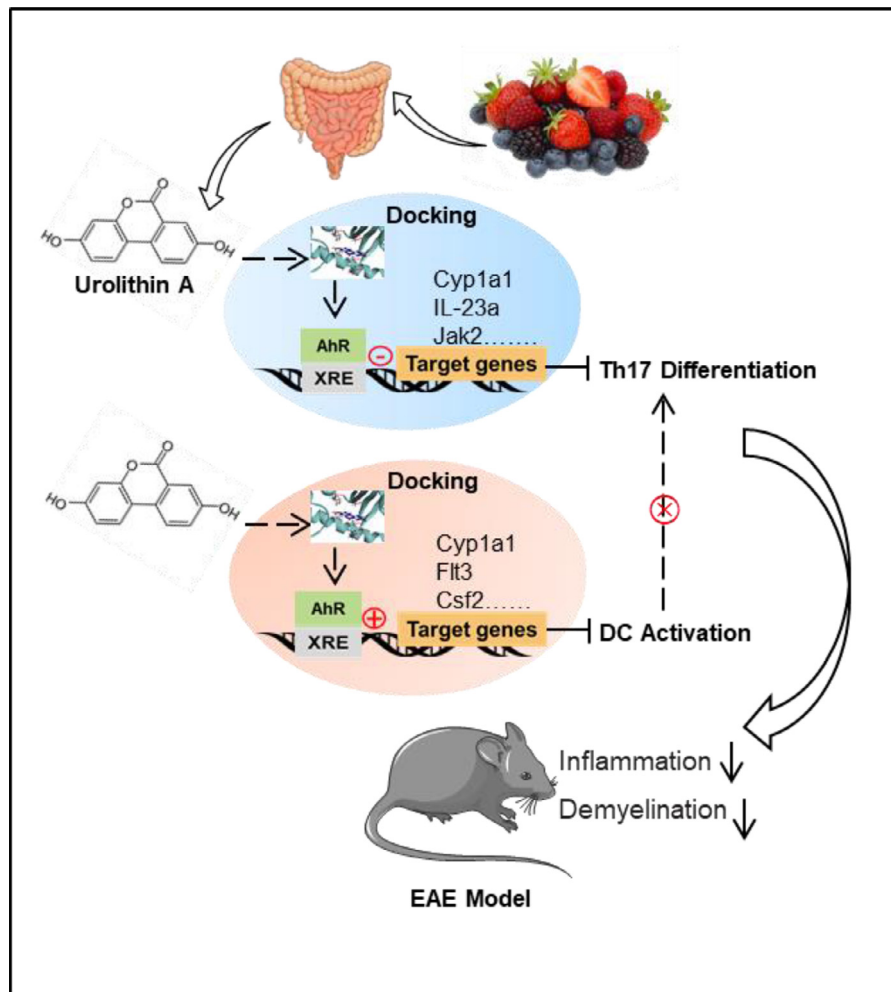
Fig. 8. *Model of URA-mediated EAE Mitigation by Directly Targeting Aryl Hydrocarbon Receptor.* URA derived from berries or medical plants rich in ellagitannin and ellagic acid achieved molecular docking with AhR, and regulated AhR downstream genes in IL-17 Family Signaling Pathway and dendritic cells developmental lineage pathway, and ultimately inhibited inflammatory cell infiltration and demyelination in EAE mice.

proportion of Th1 and Th17 cells between these two groups (Fig. 3i, j). These results shown that URA blocked pathogenic T cells from entering the CNS thus inhibited inflammation. Our experimental results also showed that URA inhibited the activation of DCs acting as antigen presents in the periphery (Fig.s1).

3.4. URA suppressed activation of bone marrow-derived dendritic cells (BM-DCs) in vitro

In vivo, URA suppressed the activation of dendritic cells in both the central and peripheral immune system. To examine whether URA had the same effect *in vitro*, primary bone marrow-derived dendritic cells (BM-DCs) were isolated from the femur and tibia of healthy 8~10-wk-old C57BL/6 mice and then changed medium every three days until maturity. Cell viability assay illustrated that 1-100 μM URA had no obvious cytotoxicity against BM-DCs (Fig. 4a). Under stimulation with 100 ng/mL LPS, BM-DCs expressed higher levels of CD80, CD86 and MHCII, markers of activated DCs, while their expression was significantly inhibited under URA treatment at 25 μM (Fig. 4b, c). Therefore, URA shown potential to limit DCs activation and decrease the expression of costimulatory molecules in BM-DCs cultures. In addition, the expression level of inflammatory cytokines in the supernatant was detected by ELISA. Secretion of IL-1β, IL-6, and TNF-α was decreased, while IL-10 production was significantly increased under URA treatment. (Fig. 4d). Furthermore, URA reduced the gene expression of IL-1β, IL-6, and iNOS, while increased the

transcriptional level of anti-inflammatory factor IL-10 (Fig. 4e). Similarly, URA exerts immunomodulatory effect on SIM-A9 microglia cell line *in vitro*, which inhibited the expression of pro-inflammatory factors TNF-α, IL-1β, IL-6, iNOS, TGF-β and up-regulated the expression of anti-inflammatory factor IL-10 (Fig. s2).

There was sufficient evidences confirmed that the antigen-presenting ability of activated dendritic cells was closely related to the differentiation of Th subsets [29−31]. Thus we explored whether URA treatment can further inhibit Th17 cell differentiation by inhibiting DC activation in the DC-CD4$^+$ T cell co-culture system. Naïve CD4$^+$ T cells isolated from C57BL/6 mice were co-cultured with URA pre-treated/untreated DCs in the activated state, and cells were assembled for flow cytometry analysis 72 h later. Results showed that compared with the vehicle group, URA pre-treated DCs significantly reduced the promotion of IL-17 secretion, while IFN-γ production wasn't influenced (Fig. 4f, g). Collectively, URA treatment suppressed the activation of DCs and weakens the antigen presentation ability.

3.5. URA restricted Th17 polarization in vitro

It is widely accepted that Th1 and Th17 pathogenic T cells induced autoimmunity and inflammation [11, 32, 33]. To further elucidate the direct effects of URA on CD4$^+$ T cells, splenocytes were isolated from healthy 8~10-wk old C57BL/6 mice and treated with URA. Cell viability assay showed that 1-100 μM URA had no obvious cytotoxic effect on cultured splenocytes *in vitro* (Fig. s3a). In the splenocyte culture

system, URA incubation inhibited Th17 polarization in a dose-dependently manner (Fig. s3b, c). In the TCR^{MOG} 2D2 T cell culture system, addition of URA at both 1 and 5 μM significantly inhibited Th17 cell differentiation (Fig. 5a, b). Results of ELISA assay was consistent with the flow cytometry analysis, that is IL-17 secretion was also obviously inhibited by URA in the culture supernatant (Fig. 5c). Real time-Quantitative PCR was performed on naïve CD4$^+$ T cells treated with URA or vehicle for 4 h under Th17 polarization conditions. The results indicated that 5 μM URA treatment had a great influence on Th17-related genes, especially decreased IL-17 family-related genes expression level (Fig. 5d). Collectively, we concluded that URA significantly inhibited CD4$^+$ T cells differentiation into Th17 *in vitro*.

3.6. URA inhibited pathogenicity of Th17 cells in adoptive EAE

To evaluate the therapeutic effect of URA on the encephalitogenecity of Th17 cells, at day 10 p.i., cells were obtained from spleen and draining lymph node of IL-17A-IRES-GFP mice, of which IL-17A-producing cells are GFP positive. Under Th17-differentiation medium, cells incubated with vehicle or 10 μM URA, and pulsed by MOG$_{35-55}$ peptide. 72 h later, CD4$^+$ T cells were purified and transferred into Naïve C57BL/6 recipient mice. As demonstrated in Fig. 6a, URA-treated T cells recipient mice obviously alleviated clinical disease development compared to the vehicle-treated group from day 14 post transferred (p.t.) (p < 0.001) (Fig. 6a). Similar to the clinical score, the accumulative scores also showed dramatically decrease in the URA-treated group (Fig. 6b). After the end of the experiment (day 17 p.i.), brain and spinal cords tissue were harvested from each group for fluorescence observation. Images showed there are amounts of GFP$^+$ cells in the CNS from the vehicle-treated group indicated the disease induced by the Th17 cells successfully. In the URA-treated group, the number of GFP$^+$ cells were greatly reduced (Fig. 6c, d). These data further evidenced an inhibition capacity of URA on the encephalitogenecity of MOG-specificity Th17 cells.

3.7. AhR as a direct target of URA

Singh et al. reported that URA and its analog UAS03 can enhance the intestinal barrier function and inhibit inflammation in colitis by activating AhR-Nrf2 dependent pathway [34]. Rothhammer V et al. also discussed the therapeutic potential of targeting AhR in autoimmune and neoplastic diseases of the CNS. Noting Aryl hydrocarbon receptor (AhR) is a ligand-dependent activated transcription factor, in DCs, AhR activation reduced MHCII expression and inhibited the induction of cytokines that promoted the polarization of pathogenic T cell subsets. Meanwhile, AhR priming also boost IL-22, IL-17A and IL-17F production in developing Th17 cells [35]. In our study, to investigate whether the immunomodulation effects of URA is also mediated via AhR signaling, we first confirmed the structural basis and binding affinity of URA to AhR using molecular docking. The CDocker module of Discovery Studio (version 3.5) platform was used to simulate the interface between URA and AhR. Docking results showed that the URA, as a ligand molecule, forms an intermolecular hydrogen bond with the amino acid residue SER75 of AhR. URA could also forms hydrophobic interaction with SER75, ALA79, LYS80, TYR137, and ILE154, as well as form van der Waals force with PRO55, PHE56, LEU72, TYR76, PHE83, and PHE136 of AhR. The complex is stable and the interaction energy is well scored (Fig. 7a−c). Next, we detected the expression of certified AhR-regulated genes in BM-DCs and CD4$^+$ T cells under Th17 polarization conditions. Our results demonstrated that URA inhibited the activation of DCs *via* regulated the downstream genes of AhR in the DCs developmental lineage pathway. Moreover, key genes in IL-17 Family Signaling Pathway including *IL-23a, IL-22, Ccl2* and other chemokines gene expression levels were significantly reduced under 5 μM URA treatment. These findings were showing the beneficial effect of URA on Th17

differentiation (Fig. 7d&e). Furthermore, we pretreated T cells with CH-223191, an AhR antagonist, for 4 h and then applied URA under the Th17 polarization conditions *in vitro*, and it was found that the inhibition effect of URA on Th17 differentiation was significantly abrogated by CH-223191 (Fig. 7f). Briefly, our data indicated that AhR was a direct target of URA and mediated the therapeutical effects of URA in EAE model.

4. Discussion

It is generally believed that the pathogenesis and development of MS is complex, including immune system dysfunction, myelin lesions of the CNS, genetic factors, and lifestyles. The progression of this disease can be divided into two stages, 1) the early autoimmune response to the myelin antigen in the peripheral immune system, and 2) CNS inflammatory response including demyelinating and axonal damage [36]. Currently, the disease-modifying therapy (DMT) approved by the European Medicines Agency (EMA) and US Food and Drug Administration (FDA)for multiple sclerosis included β interferons, glatiramer acetate, sphingosine 1-phosphate receptor modulators (fingolimod and siponimod), dimethyl fumarate, cladribine, teriflunomide, alemtuzumab, natalizumab, and anti-B cell monoclonal antibodies (rituximab and ocrelizumab) [13, 37]. The mechanisms of action, efficacy, and safety of these drugs are different, while the side effects and complications are also various and inevitable.

In this study, we demonstrated that URA, an intestinal microbiota metabolic product, has significant preventive and therapeutic effects on MOG$_{35-55}$-induced EAE mice at different disease stages. It is reported that URA exhibits various bioactivities. Abundant evidences have linked these properties of URA to inhibiting the proliferation of prostate cancer cells [38]. Recently, a study has also proved that URA treatment prevents obesity by enhancing the production of brown adipose tissue and inducing browning of white adipose tissue to increase energy consumption [39]. However, the therapeutic effects and mechanism of URA in autoimmune diseases have not been elucidated. Our study, for first time, demonstrated the immunomodulation effects of URA by diminished DC activation and Th17 response in EAE mice, and further substantiated by adoptive-transfer model showing the weak encephalitogenicity in URA-treated MOG-specifc Th17 cells. In the disease prevention stage (day 0 p.i.), the induction phase (day 11 p.i.) and the effector phase (day 17 p.i.), URA effectively alleviated the disease by playing a preventive and therapeutic role. Further histological and cytological evaluation showed that significantly fewer inflammatory cells, little demyelination and markedly reduced mononuclear cells (MNCs) in URA-treated mice. The numbers of inflammatory cells (infiltrating DCs and CNS-intrinsic microglia) and percentage of Th17 cells in the CNS were remarkably decreased, while the immune responses in the periphery were mildly affected. Compared with the Vehicle group, the URA-treated EAE mice tended to have the same immune homeostasis as healthy bodies. Mechanically, URA inhibited the activation of DCs and Th17 differentiation by directly targeting AhR, suppressed pro-inflammatory factor secretion, as well as up-regulate the inhibitory factor IL-10 to relieve EAE.

Considering that URA delayed the onset of EAE, we proposed that URA may suppress the immune response at an early stage, mainly by affecting the polarization of Th17 cells, which is considered as a key factor that triggers EAE. To investigate whether URA treatment regulated Th17 cell development directly, we explored on Th17 cell differentiation *in vitro* conditions. It was found that, on the one hand, URA directly inhibited Th17 cell differentiation. On the other hand, it reduced the expression of inflammatory factors (IL-6, IL-1β and IL-23) necessary for the differentiation of Th17 cells, thereby inhibiting DC activated-Th17 polarization indirectly.

URA has received attention because of its potential health promoting effects such as anti-inflammatory and cancer chemopreventive activities during the past few years, and our study has

discovered the therapeutic effect of URA for autoimmune diseases. In view of the many pharmacological activities of URA, it is necessary to understand the bioavailability and disposition of URA before it may be used in clinical treatment. Studies have shown that URA could be detected in plasma and urine at micromolar concentrations, after absorption, the phase II metabolites circulate in plasma and accumulate in urine are mainly glucuronides. i.e., urolithin A 3-O-glucuronide and urolithin A-8-O-glucuronide [40–42]. However, more studies need to be conducted regarding the impact of these compounds on ailments associated with autoimmune disorders.

Medicinal plants have the advantages of abundant sources and excellent therapeutic effects, but most natural drugs with small molecular weights target different immune/inflammatory pathways, making it difficult to find their direct targets. Our results showed that URA acts as a direct binding ligand for AhR to exert an immunomodulatory effect. It has been reported that the activation of AhR is closely related to the blockage of DCs function, and the interaction between the small molecule immunomodulator VAF347 and AhR protein is necessary to induce the immune regulation state of DCs [43, 44]. At the same time, previous studies have shown that AhR specifically induces the secretion of inflammatory cytokines such as IL-22, IL-6, and TGF-β under the Th17 polarization condition. It also proved that the lack of AhR significantly inhibited Th17 differentiation induced by IL-6 and TGF-β, indicating that AhR is an important positive regulator of Th17 cell differentiation [45, 46]. Interestingly, AhR is a ligand-specific transcription factor, so different AhR agonists might have opposing effects on inflammatory function. 6-formylindolo[3,2-b]carbazole (FICZ), an AhR agonist, exacerbated disease in a mouse model of EAE by AhR-dependent CD4$^+$ T cell acquisition of a Th17 cell phenotype [47]. However, AhR activated by its classical ligand 2,3,7,8-tetrachlorodibenzo-p-dioxin (TCDD) induced functional Treg cells that suppressed EAE [48]. Additionally, administration of 2-(1′ H-indole-3′-carbonyl)-thiazole-4-carboxylic acid methyl ester (ITE), another reported AhR agonist, on the day of EAE induction suppressed disease development, and draining lymph node cells from ITE-treated mice secreted lower amounts of IFN-γ and IL-17 upon activation with MOG$_{35-55}$ [49]. Our study illustrated that URA, as an ideal partial agonist of AhR, hindered the antigen uptake and presentation of DCs and inhibited Th17 polarization, thereby hindering the development of EAE.

Taken together, the *in vivo* and *in vitro* data here confirmed that as a partial agonist of AhR, URA targeted the inhibition of Th17 differentiation as well as the activation of DCs to reduce the inflammation level of EAE mice (Fig. 8). Our data displayed that URA, with wide spectrum of pharmacological activities, the low cost and the abundant sources, has encouraging therapeutic potential for autoimmune diseases such as MS.

4.1. Caveats and limitations

Our results exhibited a novel role for URA in autoimmune diseases by targeting AhR.

Although molecular docking and *in vitro* pharmacological results corroborated the role of URA as an agonist of AhR to inhibit Th17 differentiation, and thus mitigated disease progression in EAE, AhR is a ligand-specific receptor with complex functions and extensive effects, therefore, more *in vivo* evidence is needed to support our conclusions. Besides, pharmacokinetic evidences such as drug absorption, distribution, and metabolism need to present before applying URA in clinical setting.

5. Research in context

5.1. Evidence before this study

Multiple Sclerosis (MS), with high disability rate, is characterized by inflammatory cell infiltration and demyelination. It was generally accepted that helper T cell subsets, Th17 cells, were pro-inflammatory

cell groups proven to be responsible for inducing autoimmune diseases and inflammatory processes. In recent years, the application of plant-derived natural anti-inflammatory compounds in autoimmune diseases has attracted attention and achieved certain results.

5.2. Added value of this study

In this study, we demonstrated that URA had significant preventive and therapeutic effects on MOG$_{35-55}$-induced EAE mice at different disease stages, and remarkably reduced mononuclear cells (MNCs) in the central nervous system (CNS), while the immune response in the periphery were mildly affected. URA treatment suppressed the activation of bone marrow-derived dendritic cells (BM-DCs) *in vitro*, inhibited pro-inflammatory factor secretion of SIM-A9 microglia, as well as dampening Th17 cell differentiation. Furthermore, we confirmed the weak pathogenicity of URA-treated MOG-specific Th17 cells via an adoptive transfer model. Mechanistic study revealed that the inhibition effect of URA on Th17 differentiation was AhR-dependent.

5.3. Implications of all the available evidence

Our data indicates that URA - with its wide spectrum of pharmacological activities, low cost, and abundant sources - has encouraging therapeutic potential for the treatment of autoimmune diseases such as MS.

Contributors

Yuan Zhang and Xing Li conceived and designed the experiments. Pei-Xin Shen, Li Zhao, Si-Ying Deng and Yan-Yan Zhang carried out the experiments. Pei-Xin Shen, Xin Deng, Bing Han, Jie Yu and Yin Li analyzed data and wrote the manuscript. Zhe-Zhi Wang and Yuan Zhang co-supervised the study and revised the paper. All authors read and approved the final manuscript.

Data sharing statement

All data associated with this study are available in the main text or the Supplemental materials.

Declaration of Competing Interest

None of the authors have conflicts of interest.

Acknowledgments

Supplementary materials

Supplementary material associated with this article can be found in the online version at doi:10.1016/j.ebiom.2021.103227.

References

[1] Correale J, et al. Progressive multiple sclerosis: from pathogenic mechanisms to treatment. Brain 2017;140(3):527–46.
[2] Lassmann H, Bradl M. Multiple sclerosis: experimental models and reality. Acta Neuropathol 2017;133(2):223–44.

[3] Bing SJ, et al. Protective effects on central nervous system by acidic polysaccharide of panax ginseng in relapse-remitting experimental autoimmune encephalomyelitis-induced SJL/J Mice. Am J Chin Med 2016;44(6):1099–110.

[4] Smith AL, Cohen JA, Hua LH. Therapeutic targets for multiple sclerosis: current treatment goals and future directions. Neurotherapeutics 2017;14(4):952–60.

[5] Lubetzki C, et al. Remyelination in multiple sclerosis: from basic science to clinical translation. Lancet Neurol 2020;19(8):678–88.

[6] Qian C, Cao X. Dendritic cells in the regulation of immunity and inflammation. Semin Immunol 2018;35:3–11.

[[7]] Kurts C, Ginhoux F, Panzer U. Kidney dendritic cells: fundamental biology and functional roles in health and disease. Nat Rev Nephrol 2020;16(7):391–407.

[8] Giles DA, et al. CNS-resident classical DCs play a critical role in CNS autoimmune disease. J Clin Invest 2018;128(12):5322–34.

[9] Legroux L, Arbour N. Multiple sclerosis and T lymphocytes: an entangled story. J Neuroimmune Pharmacol 2015;10(4):528–46.

[10] Aranami T, Yamamura T. Th17 Cells and autoimmune encephalomyelitis (EAE/MS). Allergol Int 2008;57(2):115–20.

[11] Stromnes IM, et al. Differential regulation of central nervous system autoimmunity by T(H)1 and T(H)17 cells. Nat Med 2008;14(3):337–42.

[12] Oukka M. Interplay between pathogenic Th17 and regulatory T cells. Ann Rheum Dis 2007;66(3):iii87–90 Suppl(Suppl 3).

[13] Ontaneda D, et al. Early highly effective versus escalation treatment approaches in relapsing multiple sclerosis. Lancet Neurol 2019;18(10):973–80.

[14] Thell K, et al. Oral activity of a nature-derived cyclic peptide for the treatment of multiple sclerosis. Proc Natl Acad Sci U S A, 2016;113(15):3960–5.

[15] Rengasamy KRR, et al. The role of flavonoids in autoimmune diseases: therapeutic updates. Pharmacol Ther 2019;194:107–31.

[16] Lee MJ, et al. Oriental medicine samhwangsasim-tang alleviates experimental autoimmune encephalomyelitis by suppressing Th1 cell responses and upregulating treg cell responses. Front Pharmacol 2017;8:192.

[17] DaSilva NA, et al. Pomegranate ellagitannin-gut microbial-derived metabolites, urolithins, inhibit neuroinflammation in vitro. Nutr Neurosci 2019;22(3):185–95.

[18] Kang I, et al. Improvements in metabolic health with consumption of ellagic acid and subsequent conversion into urolithins: evidence and mechanisms. Adv Nutr 2016;7(5):961–72.

[19] Yuan T, et al. Pomegranate's neuroprotective effects against Alzheimer's disease are mediated by urolithins, its ellagitannin-gut microbial derived metabolites. ACS Chem Neurosci 2016;7(1):26–33.

[20] Piwowarski JP, et al. Role of human gut microbiota metabolism in the anti-inflammatory effect of traditionally used ellagitannin-rich plant materials. J Ethnopharmacol 2014;155(1):801–9.

[21] Bialonska D, et al. Urolithins, intestinal microbial metabolites of Pomegranate ellagitannins, exhibit potent antioxidant activity in a cell-based assay. J Agric Food Chem 2009;57(21):10181–6.

[22] Gong Z, et al. Urolithin A attenuates memory impairment and neuroinflammation in APP/PS1 mice. J Neuroinflammation 2019;16(1):62.

[23] Velagapudi R, et al. Induction of autophagy and activation of SIRT-1 deacetylation mechanisms mediate neuroprotection by the pomegranate metabolite Urolithin A in BV2 microglia and differentiated 3D human neural progenitor cells. Mol Nutr Food Res 2019;63(10):e1801237.

[24] Li X, et al. Neural stem cells engineered to express three therapeutic factors mediate recovery from chronic stage CNS autoimmunity. Mol Ther 2016;24(8):1456–69.

[25] Yang J, et al. Accelerated and enhanced effect of CCR5-transduced bone marrow neural stem cells on autoimmune encephalomyelitis. Acta Neuropathol 2012;124(4):491–503.

[26] Wang LM, et al. Nr4a1 plays a crucial modulatory role in Th1/Th17 cell responses and CNS autoimmunity. Brain Behav Immun 2018;68:44–55.

[27] Li X, et al. Carnosol modulates Th17 cell differentiation and microglial switch in experimental autoimmune encephalomyelitis. Front Immunol 2018;9:1807.

[28] Gil-Pulido J, Zernecke A. Antigen-presenting dendritic cells in atherosclerosis. Eur J Pharmacol 2017;816:25–31.

[29] Yang Y, et al. Berberine suppresses Th17 and dendritic cell responses. Invest Ophthalmol Vis Sci 2013;54(4):2516–22.

[30] Bourque J, Hawiger D. Immunomodulatory bonds of the partnership between dendritic cells and T cells. Crit Rev Immunol 2018;38(5):379–401.

[31] Fu Y, et al. NLRC3 expression in dendritic cells attenuates CD4(+) T cell response and autoimmunity. Embo j 2019;38(16):e101397.

[32] Dusi S, et al. LFA-1 controls Th1 and Th17 motility behavior in the inflamed central nervous system. Front Immunol 2019;10:2436.

[33] Bellone M, Brevi A, Huber S. Microbiota-Propelled T Helper 17 cells in inflammatory diseases and cancer. Microbiol Mol Biol Rev 2020;84(2).

[34] Singh R, et al. Enhancement of the gut barrier integrity by a microbial metabolite through the Nrf2 pathway. Nat Commun 2019;10(1):89.

[35] Rothhammer V, Quintana FJ. The aryl hydrocarbon receptor: an environmental sensor integrating immune responses in health and disease. Nat Rev Immunol 2019;19(3):184–97.

[36] Compston A, Coles A. Multiple sclerosis. Lancet 2008;372(9648):1502–17.

[37] The Lancet N. Essential medicines for patients with multiple sclerosis. Lancet Neurol 2019;18(12):1067.

[38] Eskra JN, Schlicht MJ, Bosland MC. Effects of black raspberries and their ellagic acid and anthocyanin constituents on taxane chemotherapy of castration-resistant prostate cancer cells. Sci Rep 2019;9(1):4367.

[39] Xia B, et al. Urolithin A exerts antiobesity effects through enhancing adipose tissue thermogenesis in mice. PLoS Biol 2020;18(3):e3000688.

[40] Piwowarski JP, et al. Phase II Conjugates of Urolithins Isolated from human urine and potential role of β-glucuronidases in their disposition. Drug Metab Dispos 2017;45(6):657–65.

[41] García-Villalba R, Espín JC, Tomás-Barberán FA. Chromatographic and spectroscopic characterization of urolithins for their determination in biological samples after the intake of foods containing ellagitannins and ellagic acid. J Chromatogr A 2016;1428:162–75.

[42] Ávila-Gálvez M, Espín JC, González-Sarrías A. Physiological relevance of the antiproliferative and estrogenic effects of dietary polyphenol aglycones versus their phase-ii metabolites on breast cancer cells: a call of caution. J Agric Food Chem 2018;66(32):8547–55.

[43] Hauben E, et al. Activation of the aryl hydrocarbon receptor promotes allograft-specific tolerance through direct and dendritic cell-mediated effects on regulatory T cells. Blood 2008;112(4):1214–22.

[44] Lawrence BP, et al. Activation of the aryl hydrocarbon receptor is essential for mediating the anti-inflammatory effects of a novel low-molecular-weight compound. Blood 2008;112(4):1158–65.

[45] Kimura A, et al. Aryl hydrocarbon receptor regulates Stat1 activation and participates in the development of Th17 cells. Proc Natl Acad Sci U S A, 2008;105(28):9721–6.

[46] Cui G, et al. Liver X receptor (LXR) mediates negative regulation of mouse and human Th17 differentiation. J Clin Invest 2011;121(2):658–70.

[47] Veldhoen M, et al. The aryl hydrocarbon receptor links TH17-cell-mediated autoimmunity to environmental toxins. Nature 2008;453(7191):106–9.

[48] Quintana FJ, et al. Control of T(reg) and T(H)17 cell differentiation by the aryl hydrocarbon receptor. Nature 2008;453(7191):65–71.

[49] Quintana FJ, et al. An endogenous aryl hydrocarbon receptor ligand acts on dendritic cells and T cells to suppress experimental autoimmune encephalomyelitis. Proc Natl Acad Sci USA, 2010;107(48):20768–73.